

NUMERICAL STUDY OF ELLIPTIC-HYPERBOLIC
DAVEY-STEWARTSON SYSTEM :
DROMIONS SIMULATION AND BLOW-UP

C. Besse[†], C.H. Bruneau[†]

[†] : *Mathématiques Appliquées de Bordeaux*
Université Bordeaux I
33405 Talence Cedex.

This paper is devoted to the numerical approximation of the elliptic-hyperbolic form of the Davey-Stewartson equations. A well suited finite differences scheme that preserves the energy is derived. This scheme is tested to compute the famous dromion 1 – 1 and dromion 2 – 2 solutions. The accuracy of Crank-Nicolson scheme is discussed and it is shown that it induces a phase error. Then, the qualitative behavior of the solutions is studied ; in particular the influence of the initial datum and of the various parameters is pointed out. Finally, numerical experiments show the existence of blow-up solutions

1. Introduction

The aim of this paper is to study numerically the behavior of the solutions of Davey-Stewartson system

$$(DS) \begin{cases} iu_t + \delta u_{xx} + u_{yy} = \chi |u|^2 u + bu\varphi_x, \\ \varphi_{xx} + m\varphi_{yy} = \sigma(|u|^2)_x, \end{cases}$$

where the constants δ , χ , b , m and σ are real. This system describes the evolution of water surface waves in presence of gravity and capillarity ^{1,2}. Following Ghidaglia-Saut ³, we classify these systems as elliptic-elliptic (E-E), elliptic-hyperbolic (E-H), hyperbolic-elliptic (H-E) and hyperbolic-hyperbolic (H-H) according to the sign of $(\delta, m) : (+, +)$, $(+, -)$, $(-, +)$ and $(-, -)$. In this paper, we restrict ourselves to the (E-H) case. As described in ⁴, the (E-H) mode needs appropriate boundary conditions. Following ⁴, we take

$$\begin{aligned} \lim_{\eta \rightarrow -\infty} \varphi(x, y, t) &= \varphi_1(\xi, t), \\ \lim_{\xi \rightarrow -\infty} \varphi(x, y, t) &= \varphi_2(\eta, t), \end{aligned}$$

where $\xi = cx - y$, $\eta = cx + y$ represent the characteristic variables, $m = -c^2$ and φ_1 and φ_2 are given functions.

Few mathematical results are known in this case. Hayashi and Hirata ⁵ show global in time existence and uniqueness of a solution $u \in L_{local}^\infty(\mathbb{R}, H^{3,0} \cap H^{0,3})$ with an hypothesis of regularity on initial data and boundary conditions, with

$$H^{m,l} = \{f \in L^2; \|(1 - \partial_{x_1}^2 - \partial_{x_2}^2)^{m/2} (1 + x_1^2 + x_2^2)^{l/2} f\| < \infty\}.$$

Moreover, they find a decay rate

$$\|u(t)\|_{L^\infty} \leq \frac{C}{(1+|t|)} (\|u_0\|_{H^{3,0}} + \|u_0\|_{H^{0,3}}).$$

More recently, always under assumption of small initial datum, Hayashi ⁶ proves the local existence and uniqueness of a solution in $C([0, T], H^{1+\epsilon, 0} \cap H^{0, 1+\epsilon})$.

On the other hand, for some values of the coefficients in (DS), the system is integrable by inverse scattering. A well-known example called DSI in the literature (see ^{7,8}) is elliptic-hyperbolic and can be written as :

$$(DSI) \quad \begin{cases} iu_t + 1/2(u_{xx} + u_{yy}) = -\sigma|u|^2u + u\varphi_x, \\ \varphi_{xx} - \varphi_{yy} = 2\sigma(|u|^2)_x. \end{cases}$$

For (DSI), the mathematical results are very complete (see Fokas-Sung ⁹) and moreover there exists a class of localized exact solutions called Dromions (see ^{8,10}).

From the numerical point of view, there are still very few results available since (DS) system has been derived only twenty years ago and mathematical and numerical studies have started in the 90^{ies}. To our knowledge, the only numerical work on DS (E-H) is the one of White and Weideman ¹¹ who use a split step spectral method on (DSI). Our goal is to derive a robust numerical scheme easy to implement and able to capture well the behavior of the solutions of DS (E-H) for various sets of parameters. In addition, we want to compute directly both u and φ associated to Dirichlet boundary conditions. We decide to split the two equations of (DS) system by relaxing the $u\varphi_x$ term. Then, we solve the nonlinear Schrödinger type equation by means of Crank-Nicolson scheme. As the second equation is hyperbolic, we write it in characteristic variables to make it easy to solve by a finite difference scheme.

To validate the scheme, we test it successfully by computing the well-known dromions. However, Crank-Nicolson scheme induces a phase error that is quantified on the linear Schrödinger equation. Then, we study the influence of the initial datum and the various parameters on the behavior of the solutions.

Finally, as blow-up phenomena can occur in some dispersive equations, we look for them in the focusing case ($\chi = -1$) when b or σ are small enough. The results show that a blow-up occurs even for a large set of values of b .

This paper is organized as follow :

In section 2, we recall some facts on the dromion solutions to DSI.

In section 3, we present our finite difference scheme

In section 4, we present some numerical experiments on dromions.

In section 5, we present some simulations that lead to think that the solution of DS (E-H) blows up in finite time for some values of the coefficients.

2. Exact solutions of DSI

Using inverse scattering methods, Fokas and Santini^{8,10} show for DSI that there exists localized coherent structures which are governed by the non trivial boundaries φ_1 and φ_2 , and call them “dromions” since they travel on the tracks (in ancient greek “dromos”) generated by the boundaries and are driven by them. They are localized traveling solutions which decay exponentially in both ξ and η , and can interact upon the movement. Contrary to solitons, they do not preserve their form upon interaction and can exchange energy. To obtain them, Fokas and Santini write (DSI) in the form

$$\begin{cases} iu_t + \Delta u + u[U_1 + U_2] = 0, \\ \varphi_\eta = -U_1 + \frac{\sigma}{2}|u|^2, \\ \varphi_\xi = -U_2 + \frac{\sigma}{2}|u|^2, \end{cases}$$

where

$$\begin{aligned} U_1 &= -\frac{\sigma}{2} \int_{-\infty}^{\xi} (|u|^2)_\eta d\xi' + u_1(\eta, t), \\ U_2 &= -\frac{\sigma}{2} \int_{-\infty}^{\eta} (|u|^2)_\xi d\eta' + u_2(\xi, t). \end{aligned}$$

Therefore, $u_1(\eta, t)$ corresponds to $-\varphi_{2,\eta}(\eta, t)$ and $u_2(\xi, t)$ to $-\varphi_{1,\xi}(\xi, t)$. As usual by inverse scattering techniques, the analytic form of dromions solutions is very hard to obtain. However, the (M, N) dromion solution, describing the interaction of $N \times M$ localized lumps, takes the following form

$$u(\xi, \eta, t) = 2X^tZY \quad (2.1)$$

with

$$\begin{aligned} X &= (C^x + I)^{-1}V \text{ is a vector of size } N, \\ Y &= (C^y + I)^{-1}W \text{ is a vector of size } M, \\ Z &= (A - \sigma I)^{-1}\rho \text{ and } \rho \text{ a } N \times M \text{ matrix,} \\ A &= \rho(C^y + I)^{-1}[(C^x + I)^{-1}\bar{\rho}]^t \text{ is a } N \times N \text{ matrix,} \end{aligned}$$

where the superscript t denotes the transpose of a matrix. The $N \times N$ matrix C^x is given by

$$(C^x)_{jk} = \frac{m_j \bar{m}_k}{\mu_j + \bar{\mu}_k} \exp [-(\mu_j + \bar{\mu}_k)(\xi - i(\mu_j - \bar{\mu}_k)t)],$$

and the $M \times M$ matrix C^y by

$$(C^y)_{jk} = \frac{l_j \bar{l}_k}{\lambda_j + \bar{\lambda}_k} \exp [-(\lambda_j + \bar{\lambda}_k)(\eta - i(\lambda_j - \bar{\lambda}_k)t)].$$

Finally,

$$\begin{aligned} (V)_j &= l_j \exp [-\mu_j(\xi - i\mu_j t)], \quad 1 \leq j \leq N, \\ (W)_j &= m_j \exp [-\lambda_j(\eta - i\lambda_j t)], \quad 1 \leq j \leq M, \end{aligned}$$

where $\lambda_j, \mu_j, l_j, m_j$ and $\rho \in \mathbb{C}$ and $\text{Re}(\lambda_i), \text{Re}(\mu_i) \in \mathbb{R}^+$. Besides, the boundary conditions are

$$u_1(\eta, t) = 2\partial_\eta(Y^t\bar{W}), \quad (2.2)$$

$$u_2(\xi, t) = 2\partial_\xi(X^t\bar{V}), \quad (2.3)$$

which can be written as

$$u_1(\eta, t) = -2\partial_\eta \sum_{k=1}^M \bar{m}_k \exp[-\bar{\lambda}_k(\eta + i\bar{\lambda}_k t)] Y_k(\eta, t),$$

$$u_2(\xi, t) = -2\partial_\xi \sum_{j=1}^L \bar{l}_j \exp[-\bar{\mu}_j(\xi + i\bar{\mu}_j t)] X_j(\xi, t).$$

Then, as $t \rightarrow \pm\infty$, $u_1(\eta, t)$ (resp. $u_2(\xi, t)$) consists of M (resp. L) solitons each traveling with velocity $-2\text{Im}(\lambda_k)$ (resp. $-2\text{Im}(\mu_j)$). Moreover, always as $t \rightarrow \pm\infty$, $u(\xi, \eta, t)$ consists of M times N widely separated lumps, named μ_{kj} , $k = 1..M, j = 1..N$, each traveling with velocity $(-2\text{Im}(\lambda_k), -2\text{Im}(\mu_j))$. In the special case of $\rho_{kj} = 0$ for $k \neq j$, the number of lumps is $\min(M, N)$.

To illustrate these formula, we give here the $(1-1)$ dromion expression. Let $\lambda = \lambda_R + i\lambda_I$, $\mu = \mu_R + i\mu_I$, $\hat{\xi} = \xi + 2\mu_I t$, $\hat{\eta} = \eta + 2\lambda_I t$, $\bar{\eta} = \frac{1}{\lambda_R} \ln \frac{|\lambda|}{\sqrt{2\lambda_R}}$, $\bar{\xi} = \frac{1}{\mu_R} \ln \frac{|\mu|}{\sqrt{2\mu_R}}$, $R_u = \lambda_R(\hat{\eta} - \bar{\eta}) + \mu_R(\hat{\xi} - \bar{\xi})$ and $I_u = -(\lambda_I \hat{\eta} + \mu_I \hat{\xi}) + (|\mu|^2 + |\lambda|^2)t + \arg(lm)$, then

$$u_1(\eta, t) = \frac{2\lambda_R^2}{\cosh(\lambda_R(\hat{\eta} - \bar{\eta}))^2}, \quad (2.4)$$

$$u_2(\xi, t) = \frac{2\mu_R^2}{\cosh(\mu_R(\hat{\xi} - \bar{\xi}))^2}, \quad (2.5)$$

and

$$u = \frac{4\rho\sqrt{\lambda_R\mu_R} \exp\{-R_u + iI_u\}}{(1 + \exp(-2\lambda_R(\hat{\eta} - \bar{\eta}))) (1 + \exp(-2\mu_R(\hat{\xi} - \bar{\xi}))) + |\rho|^2}. \quad (2.6)$$

The dromion solutions are not the only explicit solutions of DSI. Indeed, recently, Hietarinta and Hirota¹² and Jaulent et al.¹³ obtained a broader class of dromion solutions in terms of Wronskian determinants. Finally, Gilson and Nimmo¹⁴ considered an alternative direct approach which uses a formulation of the solutions as grammian determinants to obtain a much broader class of solutions (plane-wave solitons, dromions, solitoffs).

3. Numerical scheme

In this section, we introduce the numerical method used to compute solutions of the slightly modified (DS) (E-H) system to see the influence of each derivative term

on the behavior of the solution

$$\begin{cases} iu_t + \delta u_{xx} + \gamma u_{yy} = \chi |u|^2 u + bu\varphi_x, & (a) \\ \varphi_{xx} - c^2 \varphi_{yy} = \sigma (|u|^2)_x, & (b) \\ \lim_{\eta \rightarrow -\infty} \varphi(x, y, t) = \varphi_1(\xi, t), \\ \lim_{\xi \rightarrow -\infty} \varphi(x, y, t) = \varphi_2(\eta, t), \\ u(t=0, x, y) = u_0(x, y). \end{cases} \quad (3.7)$$

with $\delta, \gamma > 0$. Approximating this system, we face several difficulties ; namely, the size of the domain, the coupling of equations and the hyperbolic type of the second equation. Then, we have two possibilities for the numerical treatment of (3.7). On one hand, we can use the structure of the system as in ¹¹ and write (3.7) as

$$iu_t + \delta u_{xx} + \gamma u_{yy} = \chi |u|^2 u + buV$$

where

$$V = \frac{\sigma}{4c} \left(\int_{-\infty}^{\xi} (|u|^2)_{\eta} d\xi' + \int_{-\infty}^{\eta} (|u|^2)_{\xi} d\eta' \right) + \varphi_{1\xi} + \varphi_{2\eta}$$

however, without the use of spectral methods, the integrals are difficult to compute and, with such a formulation, it is not possible to compute φ . On the other hand, we can approximate separately both equations of (3.7) which is more appropriate for finite difference schemes.

Moreover, we want to preserve the energy

$$M(u) = \int_{\mathbb{R}^2} |u|^2 dx dy \quad (3.8)$$

3.1. Semi-discretization in time

The main idea is to use the Crank-Nicolson scheme proposed by Delfour-Fortin-Payre ¹⁵ for the nonlinear Schrödinger equation (NLS) :

$$(NLS) \quad \begin{aligned} iu_t + \Delta u &= \lambda |u|^2 u \quad , \quad x \in \mathbb{R}^d, \quad t > 0, \\ u(x, t=0) &= u_0(x) \quad , \quad x \in \mathbb{R}^d. \end{aligned}$$

This scheme is studied in ^{16,17,18}. It is fully implicit and exactly preserves both invariants of (NLS). It takes the semi-discretized form

$$i \frac{u^{n+1} - u^n}{\delta t} + \Delta \left(\frac{u^{n+1} + u^n}{2} \right) = \lambda \left(\frac{|u^{n+1}|^2 + |u^n|^2}{2} \right) \frac{u^{n+1} + u^n}{2}$$

where u^n is the approximation of u at time $t^n = n\delta t$. In fact, this equation is written at time $t^{n+\frac{1}{2}} = (n+1/2)\delta t$. In order to use this scheme for DS (E-H), we just have to add the discretization of the term $u\varphi_x$. We write it as

$$\left(\frac{u^{n+1} + u^n}{2} \right) \varphi_x^{n+\frac{1}{2}}$$

and replace the operator Δ by $D = \delta\partial_{xx} + \gamma\partial_{yy}$. Now, the principle of relaxation is to write (3.7 b) at the different time $t^n = n\delta t$, and proceeding in the same way, we obtain

$$L\left(\frac{\varphi^{n+\frac{1}{2}} + \varphi^{n-\frac{1}{2}}}{2}\right) = \sigma(|u^n|^2)_x$$

where $L = \partial_{xx} - c^2\partial_{yy}$. We take as initial condition $u^0 = u_0$. Finally, we get

$$i\frac{u^{n+1} - u^n}{\delta t} + D\left(\frac{u^{n+1} + u^n}{2}\right) = \chi\left(\frac{|u^{n+1}|^2 + |u^n|^2}{2}\right)\left(\frac{u^{n+1} + u^n}{2}\right) + b\left(\frac{u^{n+1} + u^n}{2}\right)\varphi_x^{n+\frac{1}{2}} \quad (3.9)$$

$$L\left(\frac{\varphi^{n+\frac{1}{2}} + \varphi^{n-\frac{1}{2}}}{2}\right) = \sigma(|u^n|^2)_x. \quad (3.10)$$

Then, there is conservation of the energy (3.8). Indeed, multiplying (3.9) by $\overline{u^{n+1} + u^n}$, integrating in space and taking the imaginary part, we get

$$\int_{\mathbb{R}^2} |u^{n+1}|^2 dx dy = \int_{\mathbb{R}^2} |u^n|^2 dx dy. \quad (3.11)$$

Moreover, as the functions φ_1 and φ_2 are defined on the characteristic variables, we have to rewrite (3.9) and (3.10) in the (ξ, η) plane

$$\begin{cases} S\left(\frac{\varphi^{n+\frac{1}{2}} + \varphi^{n-\frac{1}{2}}}{2}\right) = \frac{\sigma}{4c}T(|u^n|^2) & (a) \\ i\frac{u^{n+1} - u^n}{\delta t} + (c^2\delta + \gamma)\Delta\left(\frac{u^{n+1} + u^n}{2}\right) + 2(c^2\delta - \gamma)S\left(\frac{u^{n+1} + u^n}{2}\right) = & (b) \\ \left(\chi\frac{|u^{n+1}|^2 + |u^n|^2}{2} + bcT(\varphi^{n+\frac{1}{2}})\right)\left(\frac{u^{n+1} + u^n}{2}\right) & (3.12) \end{cases}$$

where $S = \partial_{\xi\eta}$ and $T = \partial_{\xi} + \partial_{\eta}$.

Remark 0.1 *In this paper, we do not prove neither existence of a solution nor the convergence of the scheme. However, the same scheme is used in ¹⁹ for the (NLS), DS (E-E) and DS (E-H) equations and results of existence and convergence of solutions are proved.*

3.2. Full discretization

For the spatial approximation, we restrict the infinite domain to a large enough bounded one and take homogeneous Dirichlet conditions on the boundary. We consider the approximated domain is large enough when the value of the initial datum at the boundary is less than 10^{-6} . The numerical tests show that this is enough to avoid a damage of the qualitative behavior of the solution.

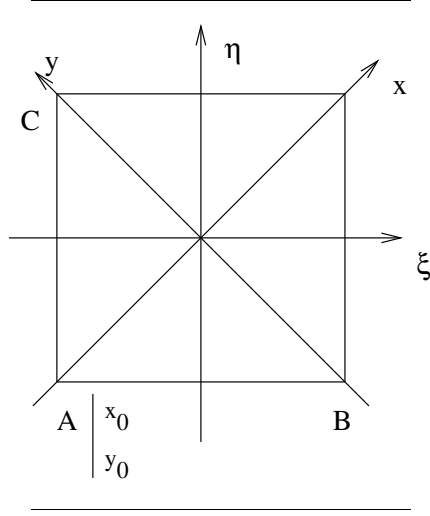


Fig. 1. Domain

The non trivial boundary conditions on the mean flow φ are well adapted to such a domain. Indeed, if we represent it on figure (1), we just have to prescribe them on (AB) and (AC) . Obviously, we will impose that $\lim_{\xi \rightarrow -\infty} \varphi_1(\xi, t) = \lim_{\eta \rightarrow -\infty} \varphi_2(\eta, t) = 0$, so that, the point A will have to be chosen sufficiently far from the origin. We mesh the bounded domain with a $(J - 1) \times (K - 1)$ grid. We will denote by δx and δy the space steps, and u_l^n the value at the point $(x_0 + (j - 1)\delta x, y_0 + (k - 1)\delta y)$, $(j = 1..J, k = 1..K)$, $l = J(k - 1) + j$, and $\varphi_l^{n+\frac{1}{2}}$ the value of φ at the same point. Always using centered finite differences, the fully discrete scheme reads

$$\left\{ \begin{array}{l}
 \frac{1}{4\delta x \delta y} \left[\frac{(\varphi_{l+1+J}^{n+\frac{1}{2}} - \varphi_{l+1-J}^{n+\frac{1}{2}} - \varphi_{l-1+J}^{n+\frac{1}{2}} + \varphi_{l-1-J}^{n+\frac{1}{2}})}{2} + \frac{(\varphi_{l+1+J}^{n-\frac{1}{2}} - \varphi_{l+1-J}^{n-\frac{1}{2}} - \varphi_{l-1+J}^{n-\frac{1}{2}} + \varphi_{l-1-J}^{n-\frac{1}{2}})}{2} \right] \\
 = \frac{\sigma}{4c} \left[\frac{|u_{l+1}^n|^2 - |u_{l-1}^n|^2}{2\delta x} + \frac{|u_{l+J}^n|^2 - |u_{l-J}^n|^2}{2\delta y} \right] \\
 i \frac{u_l^{n+1} - u_l^n}{\delta t} + (c^2\delta + \gamma) \left[\frac{(u_{l+1}^{n+1} - 2u_l^{n+1} + u_{l-1}^{n+1} + u_{l+1}^n - 2u_l^n + u_{l-1}^n)}{2\delta x^2} \right. \\
 \left. + \frac{(u_{l+J}^{n+1} - 2u_l^{n+1} + u_{l-J}^{n+1} + u_{l+J}^n - 2u_l^n + u_{l-J}^n)}{2\delta y^2} \right] \\
 + \frac{2(c^2\delta - \gamma)}{4\delta x \delta y} \left[\frac{(u_{l+1+J}^{n+1} - u_{l+1-J}^{n+1} - u_{l-1+J}^{n+1} + u_{l-1-J}^{n+1} + u_{l+1+J}^n - u_{l+1-J}^n - u_{l-1+J}^n + u_{l-1-J}^n)}{2} \right] \\
 = \left[\chi \left(\frac{|u_l^{n+1}|^2 + |u_l^n|^2}{2} \right) + bc \left(\frac{\varphi_{l+1}^{n+\frac{1}{2}} - \varphi_{l-1}^{n+\frac{1}{2}}}{2\delta x} + \frac{\varphi_{l+J}^{n+\frac{1}{2}} - \varphi_{l-J}^{n+\frac{1}{2}}}{2\delta x} \right) \right] \left(\frac{u_l^{n+1} + u_l^n}{2} \right)
 \end{array} \right.$$

We can now see that the boundary conditions are well adapted. Indeed, as

$$\varphi_{l+1+J}^{n+\frac{1}{2}} = \varphi_{l+1-J}^{n+\frac{1}{2}} + \varphi_{l-1+J}^{n+\frac{1}{2}} - \varphi_{l-1-J}^{n+\frac{1}{2}} + f(\varphi^{n-\frac{1}{2}}, u^n, \delta x, \delta y)$$

we see clearly on figure (2) that $\varphi_{l+1+J}^{n+\frac{1}{2}}$ is the only unknown for the hyperbolic

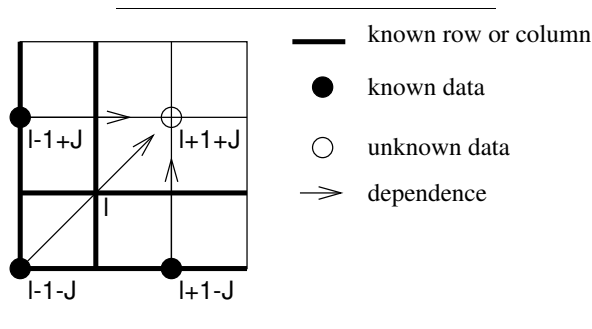


Fig. 2. Mesh

equation on φ at point l . All other terms are known from the boundary conditions or from the previous step in an explicit way going along the x -direction and then along the y -direction or conversely.

Then, the first step is to compute $\varphi^{\frac{1}{2}}$ with $S\varphi^{\frac{1}{2}} = \frac{\sigma}{4c}T(|u^0|^2)$. At each time step, we solve alternatively the hyperbolic equation (3.12-(a))

$$S\varphi^{n+\frac{1}{2}} = -S\varphi^{n-\frac{1}{2}} + \frac{\sigma}{2c}T(|u^n|^2)$$

and the equation (3.12-(b)) using a standard iteration procedure based on a fixed-point algorithm. So, we get successive approximations of u^{n+1} by solving linear systems until we estimate that there is enough precision.

4. Numerical experiments

4.1. Computation of dromion solutions

As we mentioned in section 2, there are explicit solutions of the sub case (DSI). So, we first test our scheme on (DSI) system and dromion solutions. We start with the 1-1 dromion solution

$$u(\xi, \eta, t) = \frac{4i \exp(-(\xi + \eta + 4t) - i(\xi + \eta))}{(1 + \exp(-2\xi - 4t))(1 + \exp(-2\eta - 4t)) + 1}$$

corresponding to $\sigma = -1$, $\lambda = \mu = l = m = 1 + i$ and $\rho = 1$ in (2.6). It represents a soliton moving with speed $2\sqrt{2}$ in the negative direction on the line $\xi = \eta$. The

non trivial boundary conditions associated with φ are

$$\begin{aligned}\varphi_1(\xi, t) &= -2 \tanh(\xi + 2t) + A \\ \varphi_2(\eta, t) &= -2 \tanh(\eta + 2t) + B\end{aligned}$$

where $A = B = -2$ in order that $\lim_{\xi \rightarrow -\infty} \varphi_1(\xi, t) = \lim_{\eta \rightarrow -\infty} \varphi_2(\eta, t) = 0$. Moreover, as

$$\varphi(\xi, \eta, t) = \frac{\sigma}{2} \left(\int_{-\infty}^{\eta} |u|^2(\xi, s, t) ds + \int_{-\infty}^{\xi} |u|^2(s, \eta, t) ds \right) + \varphi_1(\xi, t) + \varphi_2(\eta, t)$$

an easy computation gives

$$\varphi(\xi, \eta, t) = -4 \frac{\frac{1}{1 + \exp(2\xi + 4t)} + \frac{1}{1 + \exp(2\eta + 4t)}}{(1 + \exp(-2\xi - 4t))(1 + \exp(-2\eta - 4t)) + 1} + \varphi_1(\xi, t) + \varphi_2(\eta, t)$$

We take the initial datum at $t = -3$. The domain is the square $[-12, 12] \times [-12, 12]$ with a 128×128 mesh, $\delta t = 10^{-3}$ and $t \in [-3, 3]$. On the figures (3),(4), we plot the module of the theoretical and the numerical solution at $t = 0$.

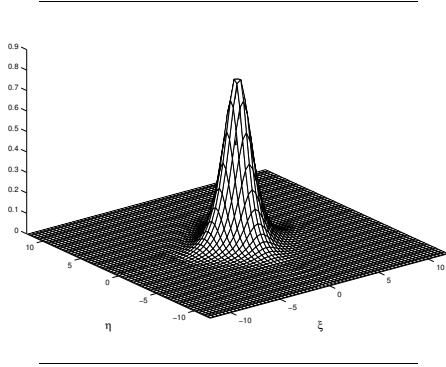


Fig. 3. Numerical dromion 1-1

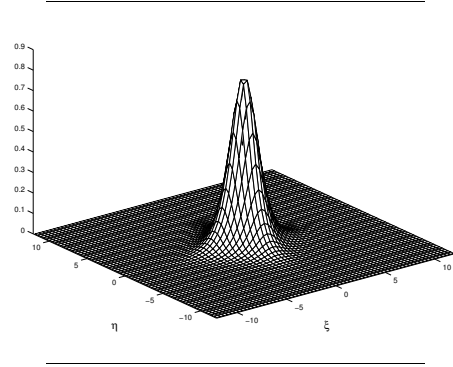


Fig. 4. Exact dromion 1-1

We can not see any relevant differences. To emphasize it, we look at the evolution of the contour of the localized solution for $t = -3, 0, 3$ on figure (5).

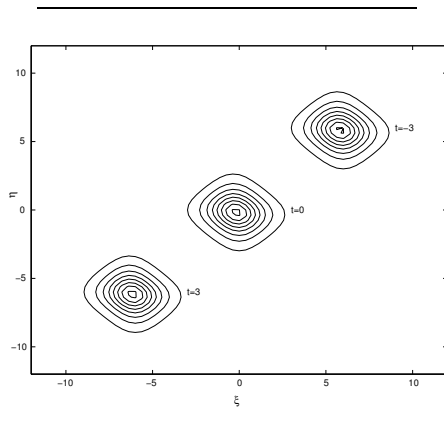


Fig. 5. Contour of numerical dromion 1-1

The structure of the dromion is perfectly preserved. Moreover, we show the evolution of the L^∞ -norm and see that it is well conserved on figure (6).

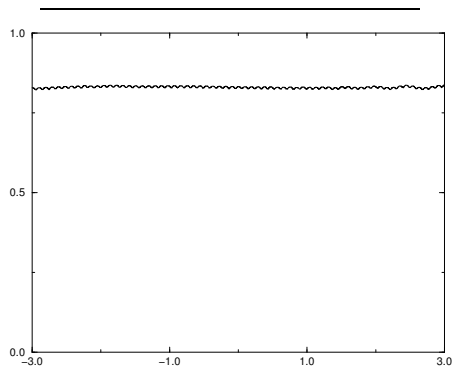


Fig. 6. L^∞ norm

Next, to understand better what driven by the tracks means, we plot φ for the same values of t on (fig(7,8,9)).

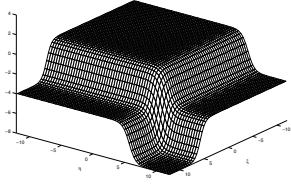


Fig. 7. φ at $t=-3$

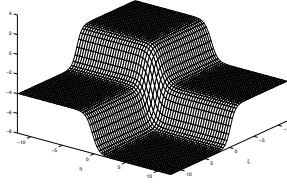


Fig. 8. φ at $t=0$

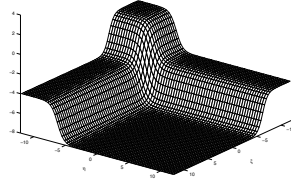


Fig. 9. φ at $t=3$

In fact, if we compare position of u on fig(5) with cross section position of the contour of φ on fig(10,11,12), we can see that u is exactly localized on the tracks left by φ .

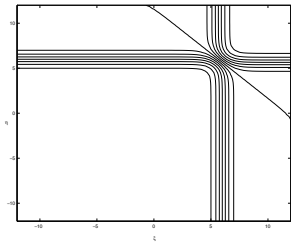


Fig. 10. φ at $t=-3$

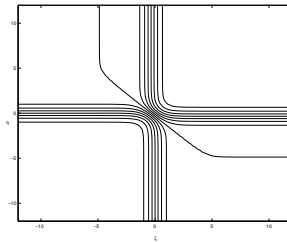


Fig. 11. φ at $t=0$

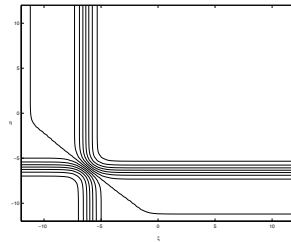


Fig. 12. φ at $t=3$

In order to analyze better the error we made, we plot on figure (13, 14, 15) $N_1 = ||u_{ex}||_2 - ||u_{num}||_2$, $N_2 = ||u_{ex} - u_{num}||_2$ and $N_3 = |||u_{ex}| - |u_{num}|||_2$ where u_{ex} is the exact solution and u_{num} the numerical one.

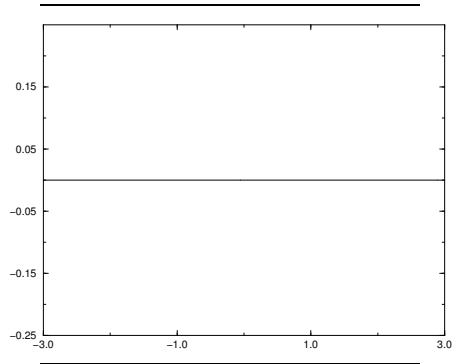


Fig. 13. $N_1 = \|u_{ex}\|_2 - \|u_{num}\|_2$

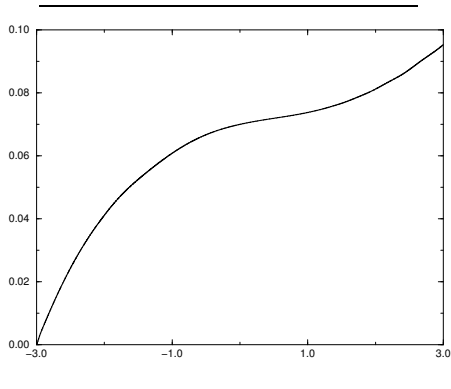


Fig. 14. $N_2 = \|u_{ex} - u_{num}\|_2$

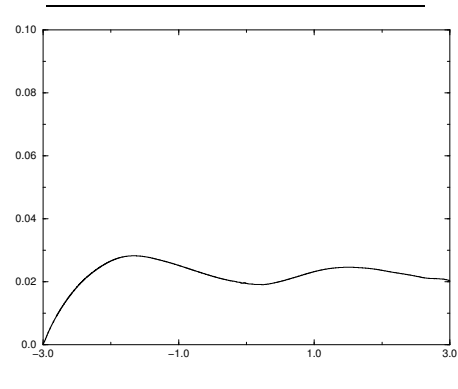


Fig. 15. $N_3 = \|||u_{ex}| - |u_{num}|\|_2$

The N_1 quantity is less than 10^{-5} at any time as expected from (3.11). However, the phase error is quite high as revealed by N_2 .

This phase error comes from the Crank-Nicolson scheme. Indeed, let us consider the linear Schrödinger equation

$$(LS) \begin{cases} i u_t + \Delta u = 0, \\ u(0, x) = u_0(x), \end{cases}$$

and the semi-discrete Crank-Nicolson schemes

$$\begin{cases} i \frac{u^{n+1} - u^n}{\delta t} + \Delta \frac{u^{n+1} + u^n}{2} = 0, \\ u^0(x) = u_0(x). \end{cases} \quad (4.13)$$

The solution of (LS) is given by

$$u(x, t) = S(t)u_0(x)$$

where $\widehat{S(t)}(\zeta) = \exp(-i\zeta^2 t)$ and $\widehat{(\cdot)}$ denotes the Fourier transform. Writing (4.13) as

$$u^{n+1} = (Op_1)^{-1}Op_2 u^n$$

with $Op_1 = (\frac{i}{\delta t} + \frac{\Delta}{2})$ and $Op_2 = (\frac{i}{\delta t} - \frac{\Delta}{2})$. We get

$$\widehat{u^{n+1}} = \exp(i\theta)\widehat{u^n} = \exp(i(n+1)\theta)\widehat{u^0}$$

with $\theta = -\zeta^2 \delta t + \frac{\zeta^6 \delta t^3}{12} + o(\zeta^{10} \delta t^5)$. Thus, if $t = n\delta t$,

$$\|u_{ex}(t) - u^n\|_2 = 2 \left| \sin\left(\frac{t\delta t^2 \zeta^6}{24}\right) \right| \|u_0\|_2$$

So, the error phase could grow up to $2\|u_0\|_2$, which is not negligible. On figure (16), we plot the relative phase error ($N_2/\|u_0\|_2$) in one dimension for $u_0(x) = \sin(6x)$, which is the eigen vector of Laplacian operator associated to the eigenvalue $k^2 = 36$ corresponding to ζ^6 in the above formula. We take $\delta t = 10^{-2}$, $\delta x = 5 \cdot 10^{-1}$ and $x \in [0, \pi]$.

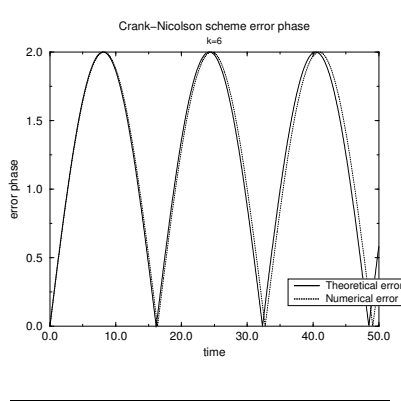


Fig. 16. Phase error for (LS) equation

Obviously, we present here the simple example to analyze the error phase of Crank-Nicolson scheme. If we want to understand why N_3 is bad too, we must plot $\| |u_{ex}| - |u_{num}| \|_2$ for a superposition of two solutions of (LS). The result for $u_0(x) = \sin(6x) + \sin(8x)$ is plotted on fig(17).

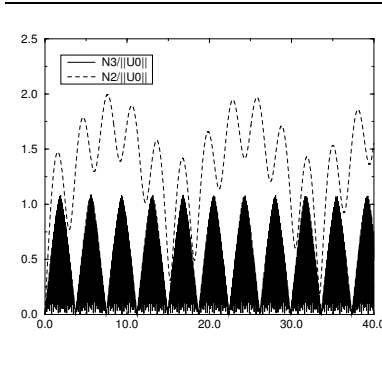


Fig. 17. $N_2/||u_0||_2$ and $N_3/||u_0||_2$ for (LS) equation

We see that the error for (LS) is quite high. In fact, $|u_{ex}| - |u_{num}|$ couples the phase as soon as the number of phase is more than two.

A possible correction for (LS) consists in solving

$$i \frac{u^{n+1} - u^n}{\delta t} + \Delta \frac{u^{n+1} + u^n}{2} + \frac{\delta t^2}{12} \Delta^3 \frac{u^{n+1} + u^n}{2} = 0$$

but, although this is better for the linear case, it is not so good for the nonlinear Schrödinger equation.

We continue our tests with the 2-2 dromion and a diagonal matrix ρ , which corresponds to the interaction of two lumps. We take $\lambda_1 = 2 - 2i$, $\lambda_2 = 4 - 0.5i$, $l_1 = 2 + 1$, $l_2 = 1 + 2i$, $\mu_1 = 1 - 2i$, $\mu_2 = 3 - 0.5i$, $m_1 = 1 + i$, $m_2 = 2 + 3i$, $\rho_{11} = 1 + i$, $\rho_{22} = 2 + 3i$ and $\rho_{12} = \rho_{21} = 0$ in (2.1) to (2.3). The resulting algebraic equations are solved by making use of MapleV. Thus, we get the explicit expression of $u(\xi, \eta, t)$, $u_1(\eta, t)$ and $u_2(\xi, t)$ which are too large to be printed in this paper. Therefore, we can compare the numerical solution computed from $u(\xi, \eta, -1)$ with the exact solution above. The space domain is $[-10, 10] \times [-10, 10]$, with 257 points in every direction and $\delta t = 10^{-3}$. We plot the contour of the exact solution and the numerical one for $t = -1, 0, 1$ (fig (18)).

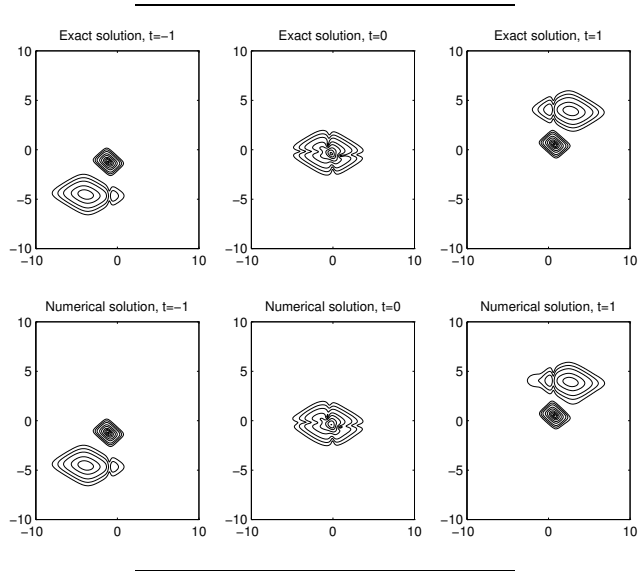


Fig. 18. Contour of dromion 2-2

The two solutions are very close to each other and we note only a small discrepancy for $t = 1$ behind the upper bump. We also draw the module of the solution (fig(19,20,21)) at the same times to show that it is really the interaction of two localized lumps.

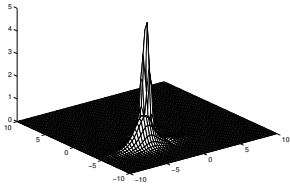


Fig. 19. Numerical dromion 2-2 at t=-1

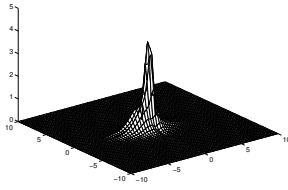


Fig. 20. Numerical dromion 2-2 at t=0

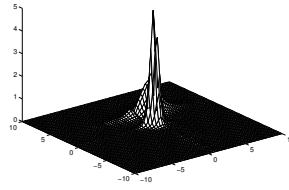


Fig. 21. Numerical dromion 2-2 at t=1

We precise the movement of the tracks left by φ with the representation of the contour of φ (fig(22,23,24)).

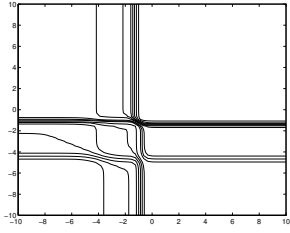


Fig. 22. φ at $t=-1$

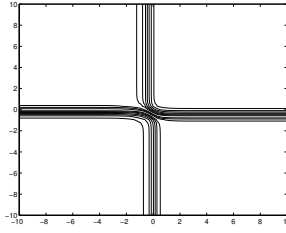


Fig. 23. φ at $t=0$

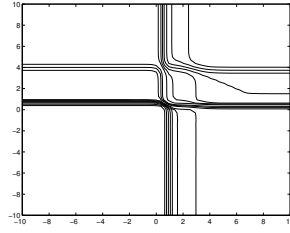


Fig. 24. φ at $t=1$

As the ρ matrix is diagonal, the number of lumps is only two instead of four. However, there are four cross-points on the tracks. Two of them localize the existing lumps and the two others give the location of the two missing ones as stated in ⁸. The phase error (fig(25)) is bigger than the one of dromion 1-1, but the dynamic of movement is more sophisticated.

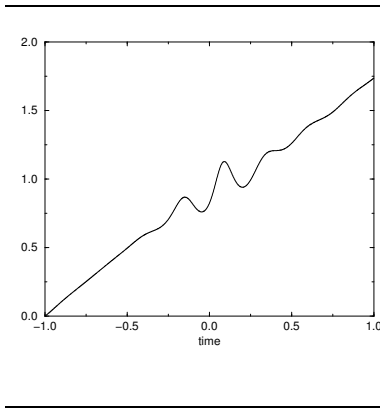


Fig. 25. $\|u_{ex} - u_{num}\|_2$

4.2. Role of the initial datum and parameters

Now that we have tested our scheme with exact solutions, we can examine the action of DS on other initial data. For that, we put the gaussian datum $u_0 = 4 \exp[-(x^2 + y^2)]$ in DSI with $\varphi_1 = \varphi_2 = 0$. Like it is stated in Fokas-Santini ⁸, all initial data with $\varphi_1 = \varphi_2 = 0$ should disperse at infinity and this is exactly what we get (fig(26,27,28,29,30)).

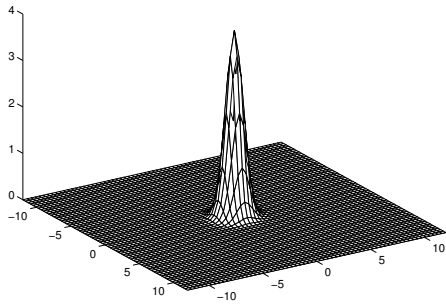


Fig. 26. Gaussian datum at $t=0$

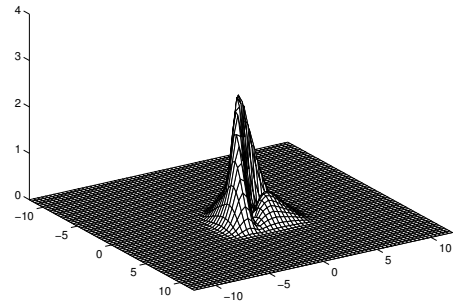


Fig. 27. Gaussian datum at $t=0.321$

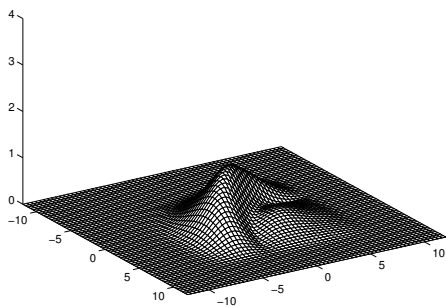


Fig. 28. Gaussian datum at $t=0.642$

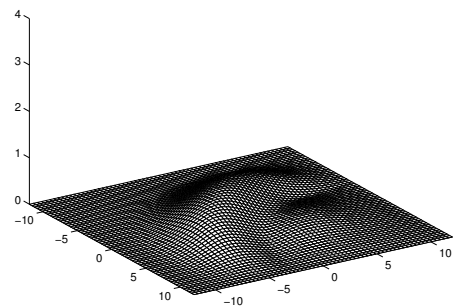


Fig. 29. Gaussian datum at $t=0.963$

We see the effect of dispersion on the L^∞ -norm which decreases with time (fig(31)).

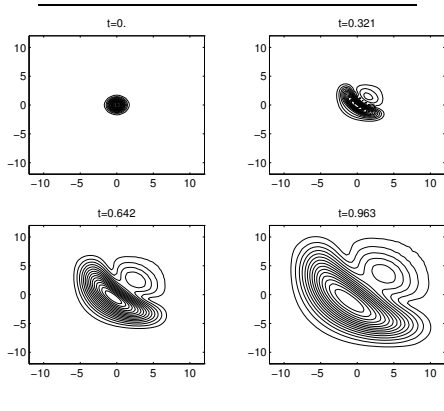


Fig. 30. Contour of gaussian datum

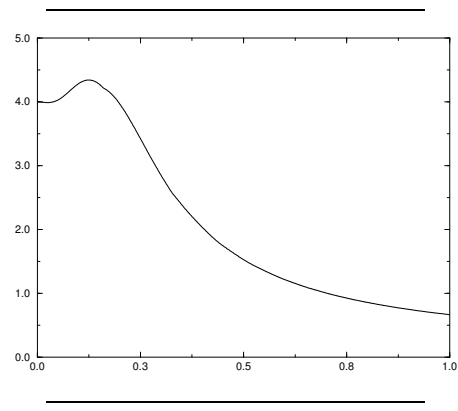


Fig. 31. L^∞ norm of gaussian datum

Then, we go on by changing some coefficients while keeping the others to the values taken for DSI. The initial datum and the boundary conditions are the same than those of dromion 1-1 test. It is difficult to make an exhaustive review of the effects of each parameter due to their number. However, we can imagine the influence of some coefficients. For example, δ and γ should manage the dispersion. Some tests show that δ and γ do not have the same influence. δ acts directly on the x -direction, whereas γ acts on the y -direction, but without the same strength. Indeed, x and y do not have the same role in DS. For example, we present here the test for $\delta = \gamma = 1$. Then, the equations become

$$\begin{cases} iu_t + \Delta u = |u|^2 u + u\varphi_x, \\ \varphi_{xx} - \varphi_{yy} = -2(|u|^2)_x. \end{cases}$$

We see that the initial lump disperses away much faster in the x -direction than in the y -direction fig(32,33).

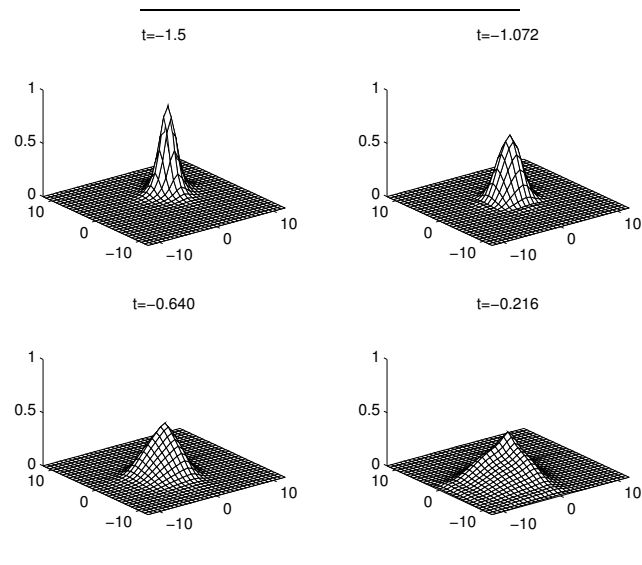


Fig. 32. $\delta = \gamma = 1$

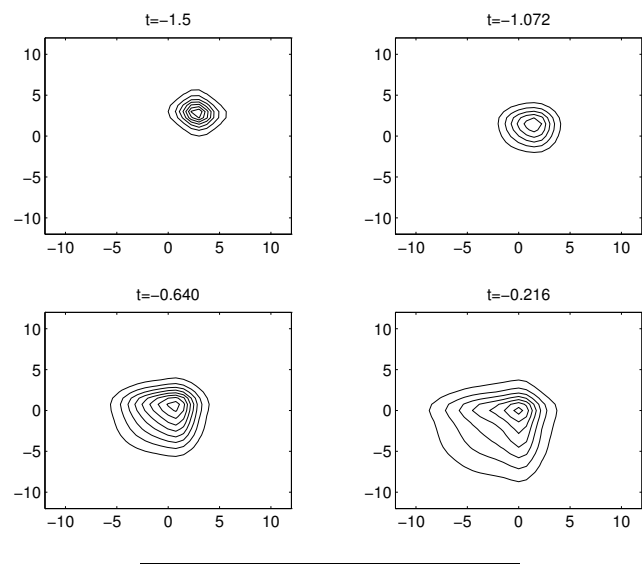


Fig. 33. $\delta = \gamma = 1$

Then, we choose to study the effects of the b parameter on the behavior of dromion 1-1. We plug into (DSI) respectively $b = 0.5$ and $b = 1.5$. We note (fig(34,35,36,37)) that dromion 1-1 is not stable at all with respect to b .

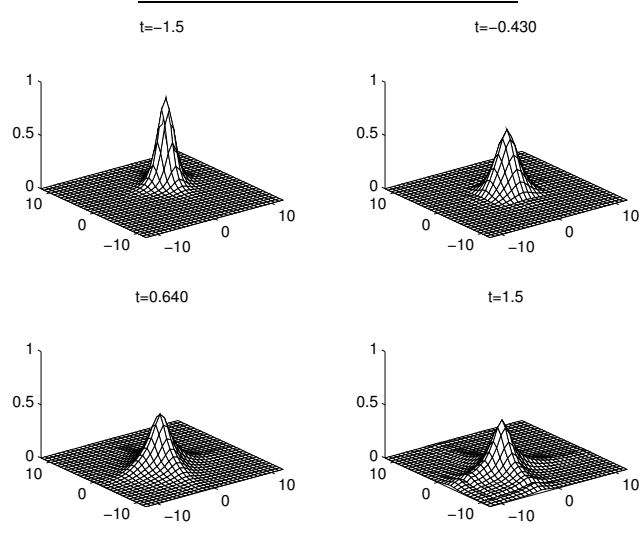


Fig. 34. $b = 0.5$

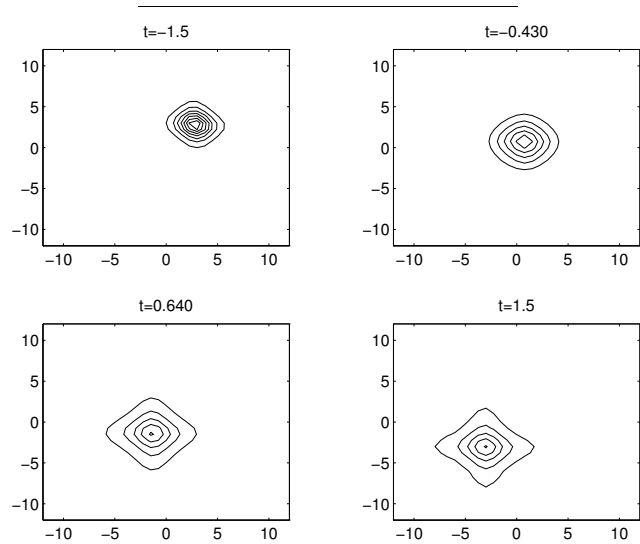


Fig. 35. $b = 0.5$

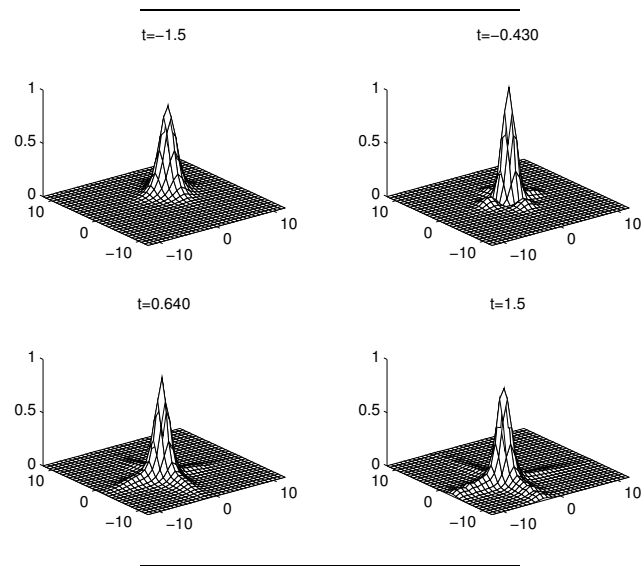


Fig. 36. $b = 1.5$

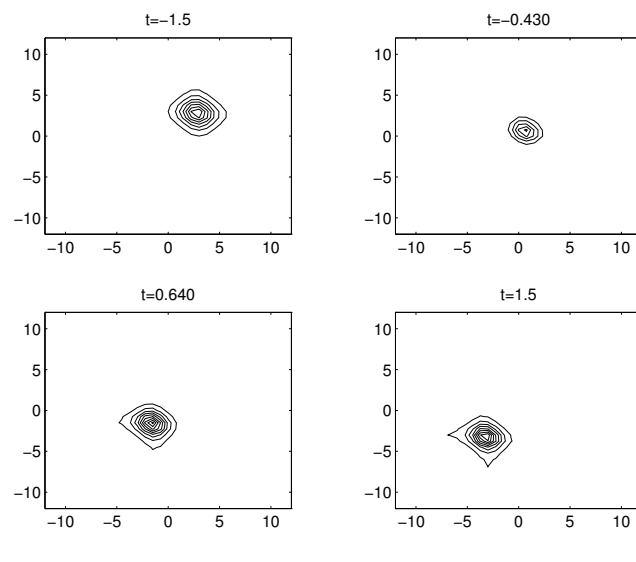


Fig. 37. $b = 1.5$

Other tests show that the results are about the same when modifying the value of χ and σ . So, dromion 1-1 is not stable with respect to the coefficients of (DSI).

5. Blow-up of DS (E-H)

It is well known that (NLS) admits blow-up solutions (see Ginibre-Velo ²⁰, Kato ²¹ or Glassey ²² for instance). Now, the dynamic of explosion is better understood (¹⁷, ²³). Moreover, as predicted by Ghidaglia and Saut ³, Papanicolaou-Sulem-Sulem and Wang ²⁴ show numerically that the blow-up occurs in the elliptic-elliptic case of (DS). Unfortunately, no results are known to validate or not the blow-up in the (E-H) mode.

From now on, we set $\delta = \gamma = 1/2$, $c = 1$ and $\varphi_1(\eta, t) = \varphi_2(\xi, t) = 0$, $\forall t$. Then, in the (ξ, η) plane, DS (E-H) becomes

$$\begin{cases} iu_t + \Delta u = \chi|u|^2u + bu\varphi_{\xi+\eta}, & (a) \\ \varphi_{\xi\eta} = \frac{\sigma}{4}(|u|_{\xi}^2 + |u|_{\eta}^2). & (b) \end{cases} \quad (5.14)$$

If we assume that $\chi = -1$, blow-up should arise when b goes to zero, as the first equation tends to the focusing (NLS) equation. In the same way, as $\sigma \rightarrow 0$, (5.14 b) gives $\varphi(\xi, \eta, t) = \psi_1(\eta, t) + \psi_2(\xi, t)$. Using the hypothesis $\varphi_1(\eta, t) = \varphi_2(\xi, t) = 0$, $\forall t$, we get $\varphi(\xi, \eta, t) = r$, $r \in \mathbb{R}$. Putting it on (5.14 a), we get exactly (NLS). Therefore, we will work finally on the system

$$\begin{cases} iu_t + \Delta u = -|u|^2u + bu\varphi_{\xi+\eta}, \\ \varphi_{\xi\eta} = \frac{\sigma}{4}(|u|_{\xi}^2 + |u|_{\eta}^2). \end{cases} \quad (5.15)$$

In order to verify our statement, we take as initial condition the one used in ¹⁷ and ²³ for blow-up of (NLS). So, $u_0 = 4 \exp[-(x^2 + y^2)]$. In the last reference ¹⁷, the presumed blow-up time for this initial datum is compute numerically and is $t_* = 0.1425$. This reference time allows us to validate our suppositions. For the numerical tests, we take a 256×256 mesh, $\delta t = 10^{-4}$ and the domain is $[-4, 4] \times [-4, 4]$.

We begin by the $\sigma - test$ consisting to compute the approximate solutions of equations (5.15), with the gaussian initial datum, for $\sigma \rightarrow 0$ and $b = 1$. We plot on fig(38) $\sup_{\xi, \eta} |u(\xi, \eta, t)|$ for different values of σ .

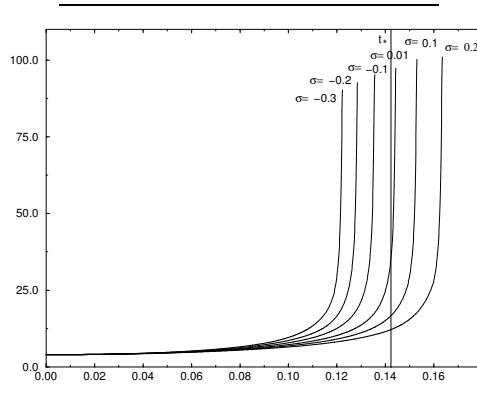


Fig. 38. Evolution of blow-up time for $b = 1$ and different values of σ

We see clearly that blow-up seems to arise and that the sign of σ changes the relative position of the blow-up time for (5.15) compared to t_* .

Next, we go on with $b \rightarrow 0$, setting $\sigma = -2$. Now, we plot the results on fig (39) for a wider range of values of b .

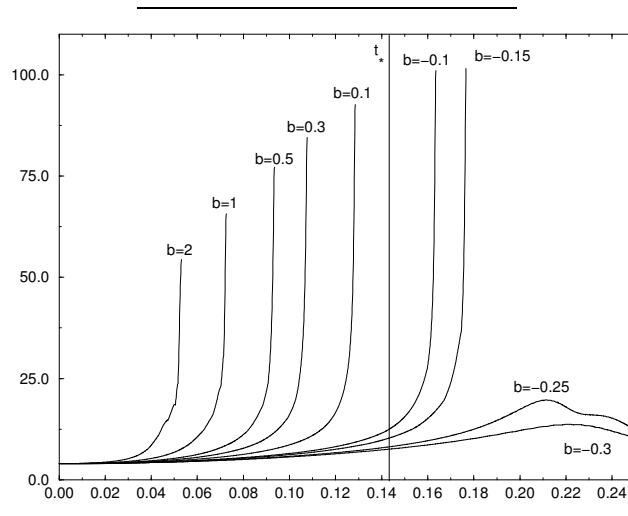


Fig. 39. Evolution of blow-up time for $\sigma = -2$ and different values of b

If b is small enough, the results are the same than for the $\sigma - test$. But we see in addition that a strong concentration and may be a blow-up occurs for values of b in $\mathcal{O}(1)$ when b is positive. Therefore, this fact seems to indicate that DS (E-H) system has an inner blow-up mechanism. For negative values of b , a stabilization

appears. The first value of b leading to this stabilization is hard to compute because of relative instability. We plot on fig (40) a more complete study on a 512×512 finer mesh for those values leading to stabilization.

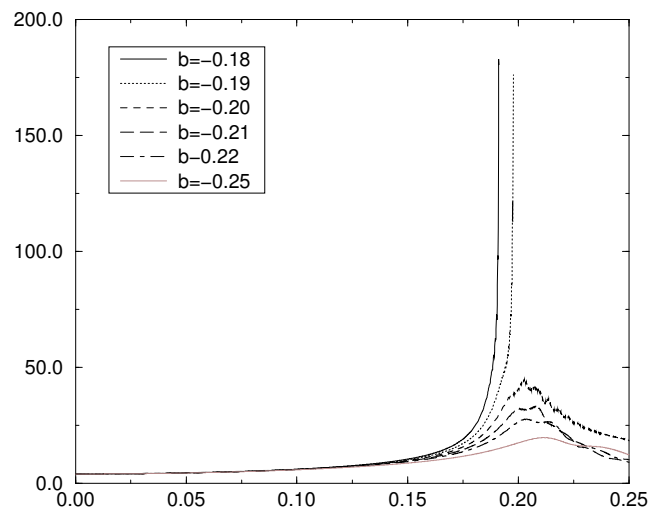


Fig. 40. Stabilization of blow-up for $\sigma = -2$

We show now that the sign of σ has an influence on the position of the supposed blow-up time of DS with respect to the blow-up time of (NLS). The fig(39) and fig(41) illustrate this fact with $\sigma = -2$ and $\sigma = +2$.

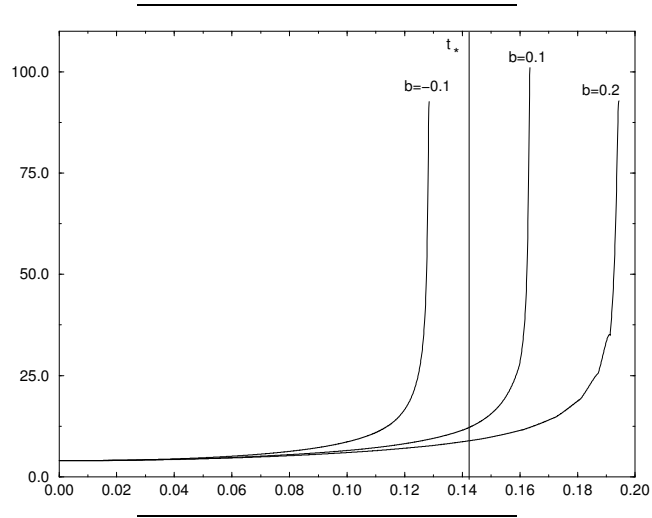


Fig. 41. Evolution of blow-up time for $\sigma = +2$ and varying b

Finally, although we do not have a refinement procedure, we show on various meshes the validity of the tests above as the L^∞ -norm increases twofold each time the mesh size is divided by two. So, we think that blow-up for DS (E-H) really exists. We plot on (fig(42)) $\sup_{\xi, \eta} |u(\xi, \eta, t)|$ for different mesh and $|u|$ (fig(43,44)) at $t = 0.1704$ for $\sigma = -2$ and $b = -0.15$.

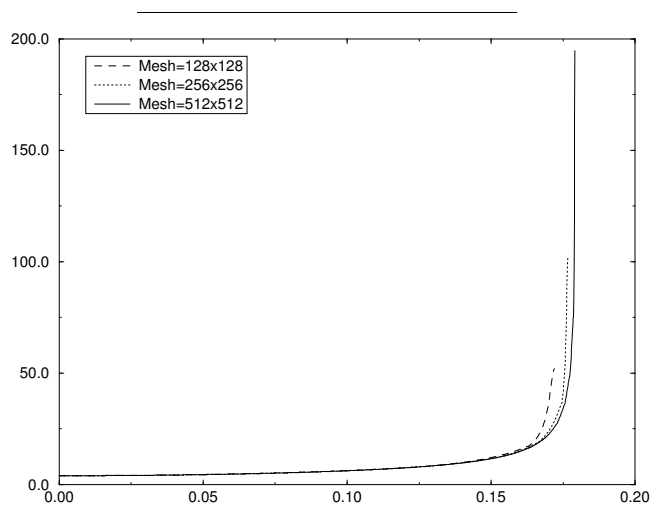


Fig. 42. Evolution of blow-up time for $b = -0.15$ and different grid mesh

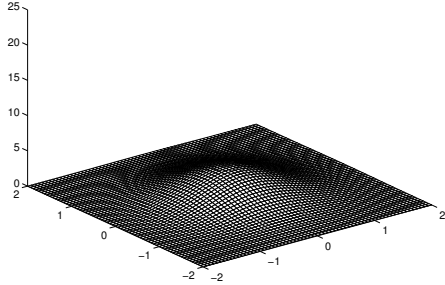


Fig. 43. $|u|$ at $t=0$

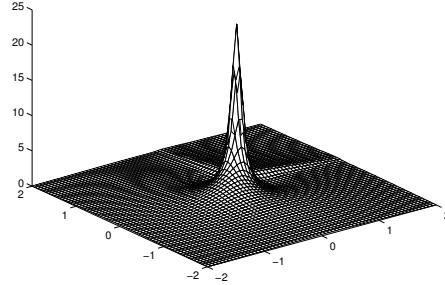


Fig. 44. $|u|$ at $t=0.1704$

6. Conclusion

We develop a new scheme in order to solve DS (E-H) systems. This tool allows to show that dromions 1-1 are not stable with respect to coefficients and that blow-up mechanism can exist for DS (E-H). We confirm that from an initial datum with $\varphi_1 = \varphi_2 = 0$, the solution disperses away for (DSI). In addition, we prove that Crank-Nicolson type schemes create a periodic phase error that can be quite big for some values of t . Unfortunately, we can not prove existence of solution and the convergence of our semi-discrete scheme. However, the principle of relaxation is applicable to a wide range of systems, and, in particular, our scheme is relatively easy to transpose to other versions of DS.

Acknowledgment

The authors thank T. Colin for valuable discussions and fruitful suggestions. They also thank P. Fabrie for helping them to understand better the phase error created by Crank-Nicolson scheme. In addition, the first author is very grateful to P. Degond who kindly welcome him at the *Mathématiques pour l'Industrie et la Physique* laboratory in Toulouse.

1. Davey A. and Stewartson K. *On three-dimensional packets of surface waves*, *Proc. R. Soc. Lond. A*, vol 338, pages 101–110, 1974.
2. Djordjevic V.D. and Redekopp L.G. *On two-dimensional packets of capillary-gravity waves*, *J. Fluid Mech.*, vol 79, pages 703–714, 1977.
3. Ghidaglia J-M. and Saut J-C. *On the initial value problem for the Davey-Stewartson systems*, *Nonlinearity* 3, pages 475–506, 1990.
4. Ablowitz M.J. and Segur H. *On the evolution of packets of water waves*, *J. Fluid Mech.*, vol 92, n^o (4), pages 691–715, 1979.
5. Hayashi N. and Hirata H. *Global existence and asymptotic behavior in time of small*

- solutions to the elliptic-hyperbolic Davey-Stewartson system, Nonlinearity 9*, pages 1387–1409, 1996.
6. Hayashi N. *Local existence in time of small solutions to the Davey-Stewartson systems, Ann. Inst. Henri Poincare*, vol 65, n^o 4, pages 313–366, 1996.
 7. Boiti M., Leon J.J.-P. and Pempinelli F. *A new spectral transform for the Davey-Stewartson I equation, Phys. Lett. A*, vol 141, n^o (3-4), pages 101–107, 1989.
 8. Fokas A.S. and Santini P.M. *Dromions and a boundary value problem for the Davey-Stewartson I equation, Physica D*, vol 44, pages 99–130, 1990.
 9. Fokas A.S. and Sung L.-Y. *On the solvability of the n-wave, Davey-Stewartson and Kadomtsev-Petviashvili equations, Inverse Problems 8*, vol 5, pages 673–708, 1992.
 10. Santini P.M. *Energy exchange of interacting coherent structures in multidimensions, Physica D*, vol 41, pages 26–54, 1990.
 11. White P.W. and Weideman J.A.C. *Numerical simulation of solitons and dromions in the Davey-Stewartson system, Mathematics and Computers in Simulation*, vol 37, pages 469–479, 1994.
 12. Hietarinta J. and Hirota R. *Multidromion solutions to the Davey-Stewartson equation, Phys. Lett. A*, vol 145, n^o (5), pages 237–244, 1990.
 13. Jaulent M., Manna M. A. and Martinez Alonso L. *Fermionic analysis of Davey-Stewartson dromions, Phys. Lett. A*, vol 151, n^o (6-7), pages 303–307, 1990.
 14. Gilson R. and Nimmo J.C. *A direct method for dromion solutions of the Davey-Stewartson equations and their asymptotic properties, Proc. R. Soc. Lond. A*, vol 435, pages 339–357, 1991.
 15. Delfour M., Fortin M. and Payre G. *Finite-difference solutions of a non-linear Schrödinger equation, Journal of computational physics*, vol 44, pages 277–288, 1981.
 16. Bidégaray, B. *Invariant measures for some partial differential equations, Physica D*, vol 82, pages 340–364, 1995.
 17. Bruneau C.H., Di Menza L. and Lehner T. *Numerical simulation of nonlinear plasmas, Rapport Interne n^o 96023, Mathématiques Appliquées de Bordeaux.*
 18. Colin T. and Fabrie P. *Semidiscretization in time for nonlinear Schrödinger-waves equations, Rapport Interne n^o 96028, Mathématiques Appliquées de Bordeaux.*
 19. Besse C. *Relaxation schemes for Nonlinear Schrödinger Equations and Davey-Stewartson Systems*, To be published.
 20. Ginibre J. and Velo G. *On a class of nonlinear Schrödinger equations part I, II, J. Funct. Anal.*, vol 32, pages 1–32, 33–71, 1979.
 21. Kato T. *Nonlinear Schrödinger equations, Lectures Notes in Physics*, 345, 1988.
 22. Glassey R.T. *On the blowing-up solutions to the Cauchy problem for nonlinear Schrödinger equations, J. Math. Phys*, vol 18, n^o (9), pages 1794–1797, 1977.
 23. Sulem P.L., Sulem C. and Patera A. *Numerical simulation of singular solutions to the two-dimensional cubic Schrödinger equation, Comm. on Pure and Appl. Math.*, vol 37, pages 755–778, 1984.
 24. Papanicolaou G. C., Sulem C., Sulem P.-L. and Wang X. P. *The focusing singularity of the Davey-Stewartson equations for gravity-capillary surface waves, Phys. D*, vol 72, n^o (1-2), pages 61–86, 1994.